(EIN VERGLEICH VON METHODEN DER AKTIVEN STRÖMUNGSKONTROLLE AN EINEM SEITENLEITWERK)

A COMPARISON OF DIFFERENT ACTIVE FLOW CONTROL METHODS ON A GENERIC VERTICAL TAIL

P. Scholz, V.M. Singh,
Institute of Fluid Mechanics, TU Braunschweig, 38108 Braunschweig, Germany

A. Gebhardt
Institute of Aerodynamics and Flow Technology, German Aerospace Center
DLR, 38108 Braunschweig, Germany

S. Löffler, J. Weiss,
Institute of Aeronautics and Astronautics, TU Berlin, 10587 Berlin, Germany

Abstract

The use of Active Flow Control (AFC) methods was studied to enhance the performance of a vertical tail plane (VTP). A generic mode scale VTP was used as a joint test case to conduct, both, experiments and simulations and compare their effect and efficiency in generating additional side force at the VTP. Three different methods have been applied: vortex generating devices, tangential blowing and alternately pulsed blowing, each in some different variations and with different mass flow rate. The results show that the choice of the most efficient method is dependent on the overall effect that needs to be created: The vortex generating devices can crate small additional side force with very high efficiency. Alternately blowing pulsed jets require more mass flow rate to be operated, but can achieve larger side force. And finally the tangential blowing can generate large side forces, but eventually requires a noteworthy mass flow rate. For a given rudder deflection, an additional side force coefficient between 0.1 and 0.4 can be generated, the efficiency in terms of the lift gain factor can reach values as high as 100, if only small additional side force is required, but drops to values between 40 and 20, if larger side force is desired.

Keywords

Active Flow Control, Vertical tail plane, Separation control, Actuation methods
Aktive Strömungsbeeinflussung, Seitenleitwerk, Ablösekontrolle, Aktuatoren

1. INTRODUCTION

The vertical tail of an aircraft has to ensure stability and flight control in the whole flight envelope and under all foreseeable conditions. Most medium- to long-range jet airliners are designed as underwing-mounted twin-engine jets and as a "family" of aircrafts with different fuselage lengths, which share the same empennages. This design has impact on the sizing of the vertical tail plane (VTP), because the unsymmetrical thrust distribution during a "one engine inoperative" (OEI) event results in a large yaw moment, which must be counteracted by a aerodynamic side force of the VTP. For the smallest member of an aircraft family the moment arm of the vertical tail is shortest, such that the size is typically dominated by the requirement to maintain flight control during OEI, while other requirements (e.g. static stability and manoeuvrability in normal operation) could be met with smaller VTPs. Large vertical tails contribute undesirable weight and friction drag and it is therefore interesting to study methods to increase the effectiveness of the vertical tail.

During the OEI-event the VTP has to generate maximum side force under a side slip angle β while the rudder is deflected to a large angle δ_r. The flow over the rudder separates. Therefore, the aerodynamic task for active flow control is to reduce, or probably fully prevent, the separation over the rudder near maximum side force conditions.

A consistent study regarding the use of active flow control on a VTP was done in the framework of the Boeing eco-Demonstrator program. It ranged from conceptual studies in a low speed wind tunnel [1], over wind tunnel experiments with a full scale VTP model [2] to flight tests with a modified Boeing 757 "ecoDemonstrator" [3]. These studies have demonstrated the successful application and particularly the scaling of the method from small wind tunnels to flight tests. However, the researchers concentrated on applying a certain AFC method, namely the sweeping jets, at the vertical tail, but several other means of active and also passive flow control are known. It is yet not published, what would be the optimal choice for a certain objective and a quantitative comparison is required.

doi:10.25967/480086

Probably the most obvious flow control method is a tangential wall jet. The concept goes back to the early days of aerodynamics — soon after the process of separation (the loss of momentum in the lower boundary layer close to the wall) has been discovered, additional momentum was actively injected tangentially at the wall, such that the separation can be delayed, see references in [4], [5], [6] and [7]. The most challenging task with wall jets is to gain a suitable efficiency, and it was found that it increases substantially, if the wall jet passes over a convex surface, such that the high velocity generates a distinct low-pressure region, which contributes to the desired force. Also the outer flow stays attached to the wall jet, which is often called the "Coanda-effect". With an attentive design of the jet (e.g. slot height and velocity), the convex curvature and the surrounding airfoil, such system can generate significant lift coefficients, [6], [7], with acceptable effort.

Application of a tangential wall jet to a VTP-like flow is first published in [8], where the jet was applied to a symmetrical vertical tail airfoil, utilizing the front radius of the deflected rudder as the required convex surface. Numerical simulations of the 2D airfoil revealed that, indeed, the lift can be increased significantly with good efficiency. Also a pulsed tangential wall jet was studied and it was found that pulsing might be very beneficial for efficiency, since a similar increase of lift can be generated, but with reduced mass flow.

This concept was then extended to a 3D spanwise section in [9] with numerical simulations of an infinitely swept airfoil. In this study it was found beneficial to separate the blowing slot into different spanwise segments, because longitudinal vortices are created at the edges of the discrete slots, which contribute to the momentum rearrangement, such that a similar lift can be gained, but with reduced mass flow requirement. This seems to be particularly advantageous for swept airfoils, since the sweep facilitates the longitudinal vortices, as it was also found for vortex generators, e.g. [10] and others. Also pulsing of the wall jets was studied in [9] and again pulsing increased the efficiency.

Herein, based on these preparatory studies, an extract of results will be shown in section 3.3, where tangential blowing is applied to the full VTP configuration. The full results are published in [11].

Another relatively long-known method to control separation is to introduce longitudinal vortices, [4], [12], [13]. The vortices rearrange, both, the diffusive transport and the distribution of longitudinal momentum and, if properly arranged, can therefore make up the momentum deficit of a boundary layer close to separation. The vortices can be created with mechanical (passive) devices, e.g. triangular shaped "delta wings" or rectangular shapes placed under a certain angle in the flow inside a boundary layer, which are called vane vortex generators (VVGs). Also, pitched and skewed fluidic jets can be used, which are then called the vortex generating jets (VGJ). Such comparison was done, e.g. in [10]. For a comprehensive summary of the design aspects for VGJs, such as optimal pitch and skew angles, distances between individual vortex pairs and the relevance of the jet velocity, refer to [7], [14] and references therein.

Application of passive vortex generating devices to control the flow over a VTP has been published as a comparative case in [2]. For the configuration discussed herein, experimental data is given in [15] and [16], also comprising a comparison of the passive VVGs with active VGJs. The main findings of these experiments will be recapped in section 3.2.

It was mentioned above that it seems beneficial, if the wall jets undergo a periodic pulsing [9]. The beneficial effect of periodicity was actually discovered, e.g. in [17] and [18] and intensive research followed, refer to the comprehensive review in [19]. In practice the design of the "actuator" is crucial, i.e. the system that generates the periodicity. For model scale, eventually loudspeakers [18] or fast solenoid valves [20] can be used. However, systems with moving parts are considered critical for flight certification [21]. A review of possible solutions for the actuation is given in [22] and among the most promising ones is the fluidic oscillator, since it creates periodicity without any moving parts. Fluidic oscillators can be designed in very different ways, such that differentiation is not always straightforward. E.g. the sweeping jets used in [2] and [3] are variants of a fluidic oscillator.

Herein, a "pulsed jet actuator" is used [23], which is also a variant of a fluidic oscillator. The results have been published in [21] and will be summarized in section 3.4.

Due to the amount of possible means of flow control it seems interesting to quantitatively compare their effectiveness and efficiency on one and the same configuration. The actuators considered herein, continuous or discrete tangential wall jets, pulsed jets and the vortex generating jets, are all nonzero-net-mass-flux actuators, meaning, that a certain amount of pressurized air must be fed into the system. We have not considered zero-net-mass-flux concepts (such as plasma actuators or synthetic jets). For a nonzero-net-mass-flux actuator, basically, the mass flow rate of the pressurized air is the "effort". To compare the effort to the effectiveness, the momentum coefficient C_μ must be compared to the additional side force ΔC_Y that was created with this effort. This will be defined in section 3.1. The relevance of the momentum coefficient C_μ and the "lift gain factor" LGF to assess the efficiency is also discussed in [7].

2. JOINT TEST CASE

The joint test case is a generic representation of a vertical tail plane in model scale. The planform is shown in FIG. 1. The geometry is trapezoidal with a leading edge sweep of $\varphi_{LE} = 46°$, taper ratio $\lambda = 0.40$, aspect ratio $\Lambda = 1.71$ and consists of a fixed fin and an adjustable rudder. Symmetrical airfoils are used over the whole span. At the tip, the leading edge is slightly rounded, as shown in FIG. 1, and the tip is closed with circular arcs along the chord.

The rudder hinge line is at 67 % chord. The surface curvature over the rudder is very small, such that the cross profile of the rudder is merely a triangular shape with a circular radius around the hinge line. For all cases discussed herein the rudder is fixed at a constant deflection of $\delta_r = 30°$.

Herein, we consider a model scale vertical tail with a span of 0.85 m and a mean aerodynamic chord (c_{MAC}) of 0.5285 m. As the different studies have been done in different wind tunnels and with computational fluid dynamics (CFD), the Reynolds number based on c_{MAC} varies between $1.3 \cdot 10^6$ and $1.8 \cdot 10^6$. In all cases, the VTP is

mounted on a plain surface, to mimic a VTP mounted on the rear end of a fuselage. In CFD a symmetry plane was used, while in the experiments the root region interferes with a turbulent boundary layer of the wind tunnel floor, which is approximately of similar size relative to the VTP as the one at the rear end of a fuselage, such that this interaction can be considered to be realistic.

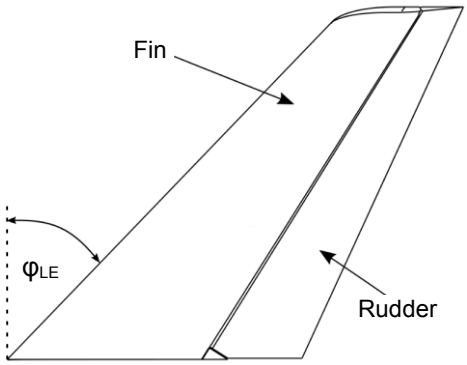

FIG. 1: Planform of the generic vertical tail

3. FLOW CONTROL METHODS

3.1. Efficiency factors

Generally speaking, for nonzero-mass-flux flow control methods, the mass flow is the main source of energy that has to be supplied by the aircraft. To assess this effort, the momentum coefficient C_μ is used. The definition is:

$$(1) \qquad C_\mu = \frac{u_j \cdot \dot{m}_j}{\frac{\rho}{2} u_\infty^2 \cdot A_{Ref.}}$$

where u_j and $\dot{m}_j$ are the jet velocity and the mass flow rate through the AFC system and the denominator is the same as for other force coefficients (such as lift, drag or side force coefficients). The numerator is basically the momentum flux and is quantitatively equivalent to the force that is introduced by the fluidic jet. In an experiment, typically $\dot{m}_j$ can be measured directly using a mass flow meter. However, u_j cannot be measured and is derived also from the mass flow rate $\dot{m}_j$ by assuming continuity and eventually introducing corrections for a compressible flow in the jet. It shall not be concealed that this process does have uncertainties, which are not yet fully assessed. They will be discussed in detail in future contributions.

Since C_μ is actually a force coefficient, it can directly be compared to the additional force coefficient generated by the action of the AFC system, ΔC_Y. The additional side force per unit momentum flux is an important assessment factor for efficiency and is called the "lift gain factor" LGF. Although originally used for lift forces, it makes as much sense to use it for the side force, which is then

$$(2) \qquad LGF = \frac{\Delta C_Y}{C_\mu} = \frac{C_{Y,Ref} - C_Y}{C_\mu}$$

LGF = 1 means, that the additional force is purely the momentum flux of the jet (similar to the thrust of a jet engine). In other words, LGF ≤ 1 is a useless AFC method. The higher the LGF, the more beneficial effect is initiated by the actuator. Apparently, the numerator in (2) requires a suited reference $C_{Y,Ref}$, the choice of which is critical to make a fair comparison of the efficiency. Therefore more aspects will be discussed in section 4.1. It is worth to note again, that all data used herein is always at a fixed rudder deflection of $\delta_r = 30°$, which is also true for all reference states $C_{Y,Ref}$. I.e. comparisons over different rudder deflection angles are *not* made.

Since C_μ is typically at least an order of magnitude smaller than the side force, it will be given in percent in the following.

3.2. Vortex generating devices

Application of vortex generating devices to the VTP has been tested in a wind tunnel with a test section size 1.3 x 1.3 m² at 57 m/s reference velocity.

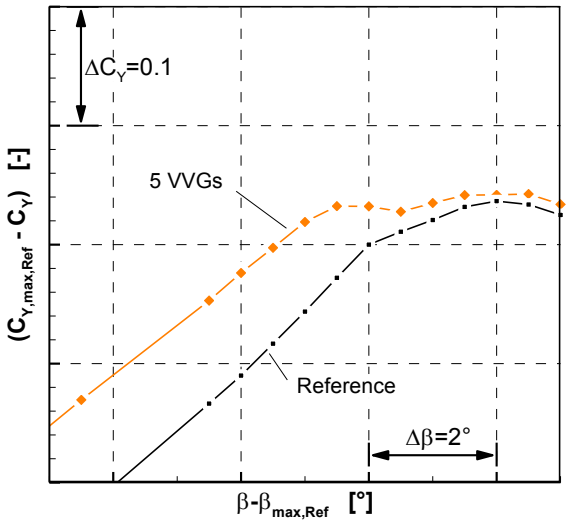

FIG. 2: Effect of VVGs on the side force

The most interesting dataset regarding the application of fixed vane vortex generators (VVGs) is shown in FIG. 2. In the test entry many different combinations, shapes, sizes, positions and orientations have been tested. As a result, five vanes attached at some small distance upstream of the hinge line have been found to be most effective. Interestingly, the VVGs are all positioned in the lower half of the span, i.e. it was found ineffective to place VVGs near the tip. Refer to [15] for a full description of the final configuration, the core result of which are shown in FIG. 2.

The VVGs enlarge the side force in the region of the linear slope. When $C_{Y,max}$ is approached, the effect reduces to rather small gains. However, considering that the VVGs are passive devices, the performance of $\Delta C_Y \approx 0.1$ in the linear range is still noteworthy.

In a second step, vortex generating jets (VGJs) have been applied with the same setup as has been found with the VVGs. That means that five jets with the same spacing, same position relative to the hinge line and a comparable orientation w.r.t. the local flow have been applied and the free parameters of this study were the diameter of the jets and the jet velocity. The full results are in [16]. It was found, that the optimum jet diameter slightly depends on β where ΔC_Y is assessed. A jet diameter of $d_j/c_{MAC} = 0.75 \cdot 10^{-3}$ may be taken as a good compromise, the results for this jet diameter with varying jet amplitude are shown in FIG. 3.

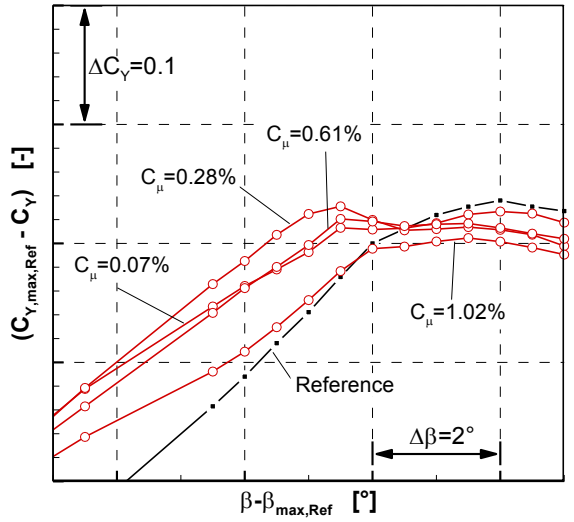

FIG. 3: Effect of VGJs with fixed jet diameter d_j and varying blowing amplitude on the side force.

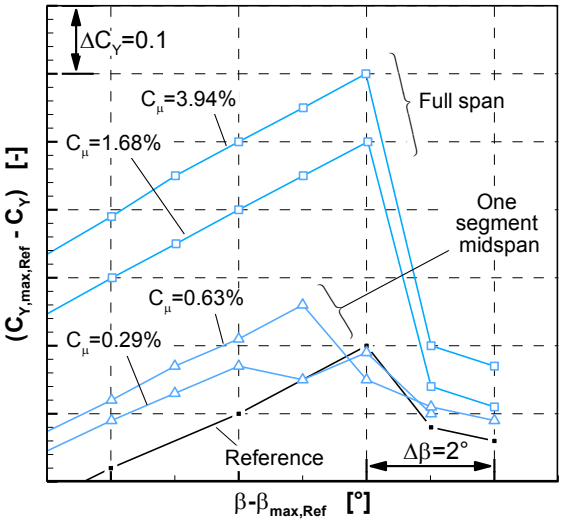

FIG. 4: Effect of tangential wall jets covering a different spanwise extent on the side force

With the correct blowing amplitude (here: $C_\mu \approx 0.28$ %), the side force curve is offset to larger C_Y in the whole β range. In contrast, for both, too strong or too weak blowing, the curve is offset only at small β, while towards $C_{Y,max}$ the benefit decreases. This is presumably due to the principle of vortex generating devices: The jet does *not* directly regain momentum in the boundary layer. Instead, a vortex is created, which in turn rearranges the momentum. This principle is bound to a sensible balance: Somewhere outside the BL enough longitudinal momentum must exist, which can be transferred. At the same time, the jet itself must not disturb the boundary layer. Both aspects become more fragile when approaching $C_{Y,max}$. Nevertheless, as found in [16], for each jet diameter a suitable blowing ratio exists that creates a linear offset of the C_Y-β-curve.

3.3. Tangential Wall Jets

The tangential wall jets were studied using numerical simulations, by solving the steady-state RANS equations with the DLR-TAU-code using a Spalart-Allmaras turbulence model including rotational corrections ("SARC"-model). Refer to [11] for more details about the numerical method. Re_{MAC} was $1.8 \cdot 10^6$ to reflect the conditions of the wind tunnel that was also used for the experiments described in section 3.2, however, only the lower wall exists and otherwise the domain is large to exclude wall interferences.

In preliminary studies, [8], e.g. the height of the blowing slot in relation to the required momentum coefficient C_μ was studied in detail using numerical simulations of a 2D airfoil. As a result, a constant slot height of $h/c = 6.6 \cdot 10^{-4}$ is used, which means, that the slot becomes smaller towards the tip of the VTP. The slot is integrated into the gap that exists, if the rudder is deflected, such that the jet blows tangentially over the circular front radius of the rudder. For what will be denoted "full span" in the following, a small region near the tip is actually not actuated, because (i) it was found ineffective and (ii) in a practical application for a model of 0.85 m span it is very hard to implement a blowing slot in this region due to the small dimensions.

FIG. 4 shows some of the results for the full VTP. If the tangential wall jets are applied over the full span, the side force can be increased by a large amount. The general character of the C_Y-β-curve is preserved, but shifted to larger C_Y-values. The required C_μ is quite significant, which is due to the combination of the large cross sectional area due to the length of the slot and relatively large jet velocity, e.g. $u_j \approx 200$m/s for $C_\mu = 1.68$%, required to achieve this effect. Other applications of tangential wall jets, e.g. [7], have gained more additional force, however, it should clearly be noted that the rudder deflection here is "only" $\delta_r = 30°$ and eventually with larger rudder deflection much larger gains could be expected.

Also shown are two results, where only a smaller segment near the middle section along span is active. Interestingly, it was found in a parameter variation, that this segment approximately at midspan is the most effective, while other segments (e.g. near the root or near the tip) are less effective for a given C_μ. This indicates, that the most sensible region regarding the separation on the rudder is somewhere around mid span. This will be picked up in section 3.4.

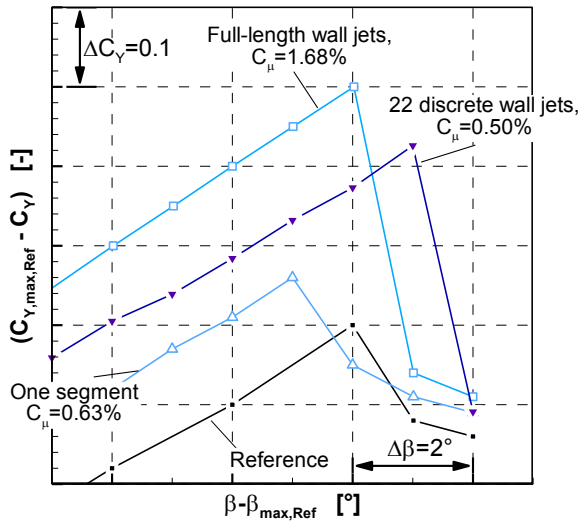

FIG. 5: Comparison of the effects of tangential jets with different spanwise extension and type

In [9] and [11] it was also found to be beneficial, if the blowing slot is not a continuous slot over the full span, but if it is separated into spanwise segments, such that the whole span is covered with 22 discrete blowing slots. The results on the VTP, compared to a continuous slot over the full length and only one segment at midspan, is shown in FIG. 5. As can be seen the discrete jets can achieve large side force with relatively low effort. E.g. roughly similar maximum side force, as compared to the full length jets, demands only one third of the C_μ.

3.4. Alternately pulsing jets

The alternately pulsing jets were tested in a wind tunnel with a test section size 2.0 x 1.44 m² at 40 m/s reference velocity.

The actuator exits are basically a sequence of 24 discrete slots embedded into the surface of the rudder, at a small distance downstream of the circular front radius. The jets exit under an angle of 30° to the local surface. Although the main component of the jets is in downstream direction, it is not a tangential wall jet, but inclined, such that it can initiate transversal vorticity that convects over the rudder and enhances the turbulent mixing. The actuator itself is a self-sustaining fluidic oscillator type: due to the internal shape of the tubing system the airflow will alternatively be guided from one exit to a neighbouring one, refer to [23]. The actuator does not feature any moving parts, the frequency of the pulsing is fixed with the internal tubing design and appears inherently, if a mass flow rate is fed through the system. The frequency, the effective amplitude u_j and the quality of the pulsing have been checked in detail and results can be found in [21], where also the results for the VTP are presented. Each actuator segment features four slots, two of which are actively blowing at a time, alternately with their respective neighbouring slot.

The results for this type of actuation with all actuators active is shown in FIG. 6. In the linear region a substantial increase of the side force can be generated. With increasing amplitude the β_{max} is slightly reduced, such that the gain of $C_{Y,max}$ is slightly smaller.

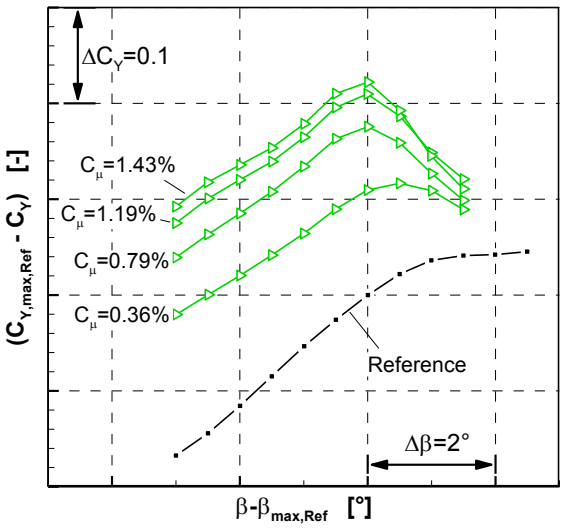

FIG. 6: Effect of 24 alternately blowing slots over full span on the lift curve

In [21] also the use of single segments was studied. For these cases not all 24 slots, but only 4 slots ("one segment") were active. Interestingly, consistent to the results in [11] for the tangential blowing, it was found to be most effective to use one segment near the midspan of the VTP, while other segments (near the tip or near the root) were found to be less effective. The data for the one-segment tangential wall jet was shown in FIG. 4 and is compared to a one segment alternately pulsing jets in FIG. 7.

The comparison is quite interesting: If we compare the two methods at roughly the same C_μ (0.29 % vs. 0.18 %), the effect for lower β is comparable, but the tangential wall jet will not be effective when approaching $\beta_{max,Ref}$. Even if the C_μ is tripled for the tangential jet, the effect in the linear region grows, but still β_{max} is reduced. In contrast, the one segment alternately pulsing jets can preserve β_{max} and $\Delta C_{Y,max}$ is similar to the tangential wall jets with three times the C_μ.

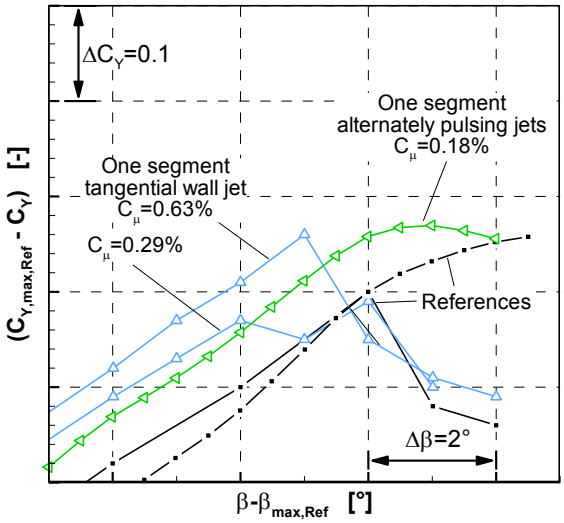

FIG. 7: Comparison between one spanwise segment near midspan with tangential wall jets vs. alternately pulsing jets.

This qualitative comparison clearly shows the necessity to assess the benefit from the AFC systems in different ways and each with respect to a suitable reference. These aspects will be discussed in the following sections.

4. COMPARISON OF THE METHODS

4.1. References without AFC

Before comparing the effect of the different methods, the different reference C_Y-β-curves are plotted in FIG. 8. Small variations exist, which can be considered typical: Note that the flow over the rudder is separated for $\delta_r = 30°$, such that a perfect match is not to be expected, if data from different wind tunnels (using different physical models of the VTP) and CFD is compared.

One characteristic feature can be seen: The data measured in wind tunnels barely shows a distinct maximal value of C_Y. Instead, beyond a certain β the slope of the C_Y-β-curve reduces. It was found for both wind tunnels (not shown here) that the drag increases rapidly beyond this

value of β, well before eventually a maximum of the side force is reached. In contrast, the data from the CFD actually shows a linear slope and then a very sudden drop of side force. This behaviour was tested (not shown here) with different turbulence models, Reynolds numbers and also with simulating the wind tunnel walls, but was found in all datasets. The full reasons for this difference between CFD and experiments cannot yet be described, however, all data *below* a certain value of β (not shown here, e.g. pressure distributions, wall shear stress visualizations, tufts, etc.) is consistent between the measurements and CFD.

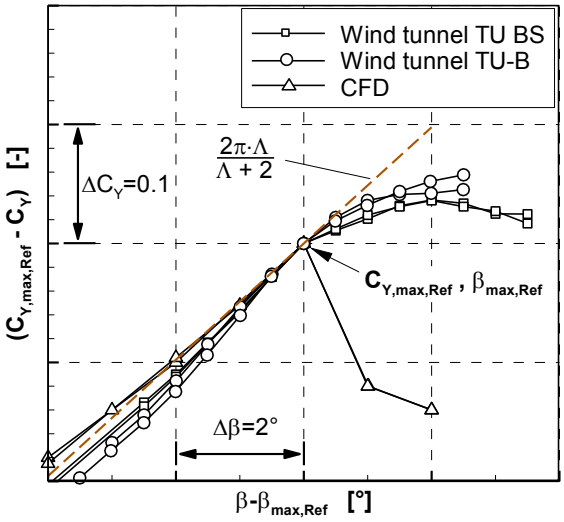

FIG. 8: Comparison of the baseline cases, VTP with δ_r=30° without flow control

For a fair comparison we have defined a certain state of the VTP to be $C_{Y,max,Ref}$ at $\beta_{max,Ref}$, which is indicated in FIG. 8. For CFD, it is the $C_{Y,max}$ actually found in the data. For the experiments we have chosen a $\beta_{max,Ref}$, where the local data (e.g. pressure distributions, etc.) is similar to what was found in CFD. It is noted, that this $\beta_{max,Ref}$ always coincided with the β-value, where the drag increases rapidly. In the following (and already done in all above figures), all data is relative to this reference state of the reference configuration.

It is noted that all data for each method was always assessed relative to its individual reference (measured in the same wind tunnel test entry, or calculated with the same geometry and the same simulation setup, respectively).

4.2. Effectiveness and efficiency

A first overview to compare the performance of the different methods is given in FIG. 9, where some C_Y-β-curves for each of the methods are plotted in the same figure. Each curve is labelled with the respective C_μ (except the VVGs, which is a passive method). Only one single reference curve is shown for orientation to not overly limit overview. The colouring of the curves for the individual methods is held consistent in the paper.

A general trend can be seen that investment of higher C_μ can increase the side force that can be achieved. This will be discussed later by quantitatively assessing the benefit and the effort for each method. In general, if β is sufficiently small, all methods offset the C_Y-β-curve to larger C_Y-values. However, FIG. 9 also shows that the effect of the different methods differs at $C_{Y,max}$ and β_{max}: Most methods reduce β_{max} w.r.t. the reference. In contrast, e.g. the discrete tangential wall jets actually give larger β_{max} and, thus, benefit also in terms of $C_{Y,max}$. Other methods differ in how much β_{max} is actually reduced and this affects also the final $C_{Y,max}$. In other words, the benefit of the methods is quite different, depending if the final $C_{Y,max}$ is of interest, or if we assess ΔC_Y somewhere in the linear region of the side force slope. Therefore, in the following, both aspect will be analyzed.

For each method, both, the ΔC_Y at one fixed β=const. in the linear region, as well as $C_{Y,max}$ was extracted relative to the individual baseline case without AFC. This data is plotted over C_μ for all cases discussed in section 3 in FIG. 10, subfigures (a) and (b). The figure is cropped to focus on the region with medium C_μ, such that one point of the tangential wall jet with highest C_μ is not shown.

For ΔC_Y in the linear region, subfigure (a), there is a clear conclusion: For low C_μ the VGJs are best able to create some additional C_Y. If one is willing to invest more C_μ, the alternately pulsing jets or the discrete tangential wall jets seem very interesting. Finally, if very large side force is required, only the full span tangential wall jet can actually achieve this.

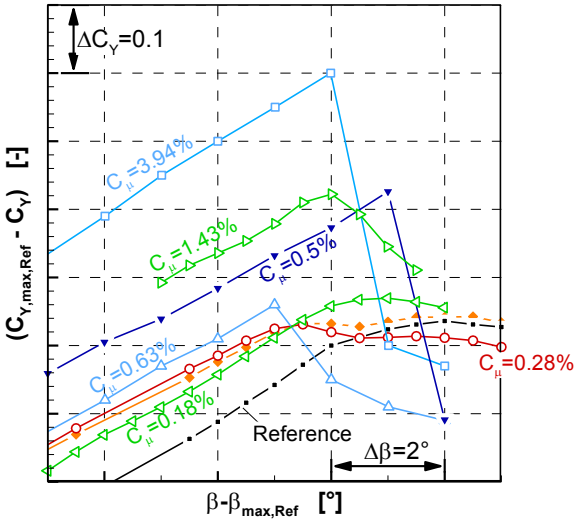

FIG. 9: Comparison of selected C_Y-β-curves of the different methods. Refer to legend in FIG. 10

The assessment is different, if we look at the values for $\Delta C_{Y,max}$ in subfigure (b): Since the vortex generating jets have a reduced β_{max}, as shown in FIG. 3, they cannot create much more maximum side force. In contrast, now the one-segment alternately pulsing jets become quite interesting in the low-C_μ-region. As noted before, it is characteristic for the discrete tangential wall jets that they actually enlarge β_{max}, which is now well visible in their $\Delta C_{Y,max}$ dominating over all other methods for medium C_μ. Again, if very large maximum side force is required, only the full span tangential wall jet can achieve it.

Yet, the comparison covered the ability to create additional side force. For technical application it is of course interesting to study the efficiency, e.g. the lift gain factor LGF introduced in section 3.1. Also the efficiency can be studied in the two ways, either for ΔC_Y at one fixed β=const. in the linear region, or for the $C_{Y,max}$ that can be achieved. This comparison is shown in FIG. 10 in subfigures (c) and (d), where the abscissa gives the effect in terms of ΔC_Y, or

$C_{Y,max}$, respectively, and the ordinate shows the efficiency as the LGF.

The general trend for most methods is that efficiency decreases with increasing demand for either ΔC_Y, or $C_{Y,max}$. This was also seen for other methods in [7] and, thus, seems to be typical. One exception is the VGJs, which are able to achieve a very large efficiency, however, only if the required ΔC_Y is small. With varying ΔC_Y or $C_{Y,max}$, different methods become more advantageous than others. Very generally speaking, for low ΔC_Y the VGJs are best and for mid ΔC_Y the alternatively pulsing jets. The full span tangential wall jet can reach very high ΔC_Y, but the efficiency is rather limited compared to other methods. Again, the discrete tangential wall jets seem to be a particularly interesting concept for medium gains of side force.

For $\Delta C_{Y,max}$ the VGJs are not so competitive for the reasons discussed above. In contrast, now the concept of a small segment of alternately pulsing jets seems extremely interesting to achieve some limited $\Delta C_{Y,max}$, but with high efficiency. With this kind of assessment now the discrete tangential wall jets are extremely interesting for medium $\Delta C_{Y,max}$.

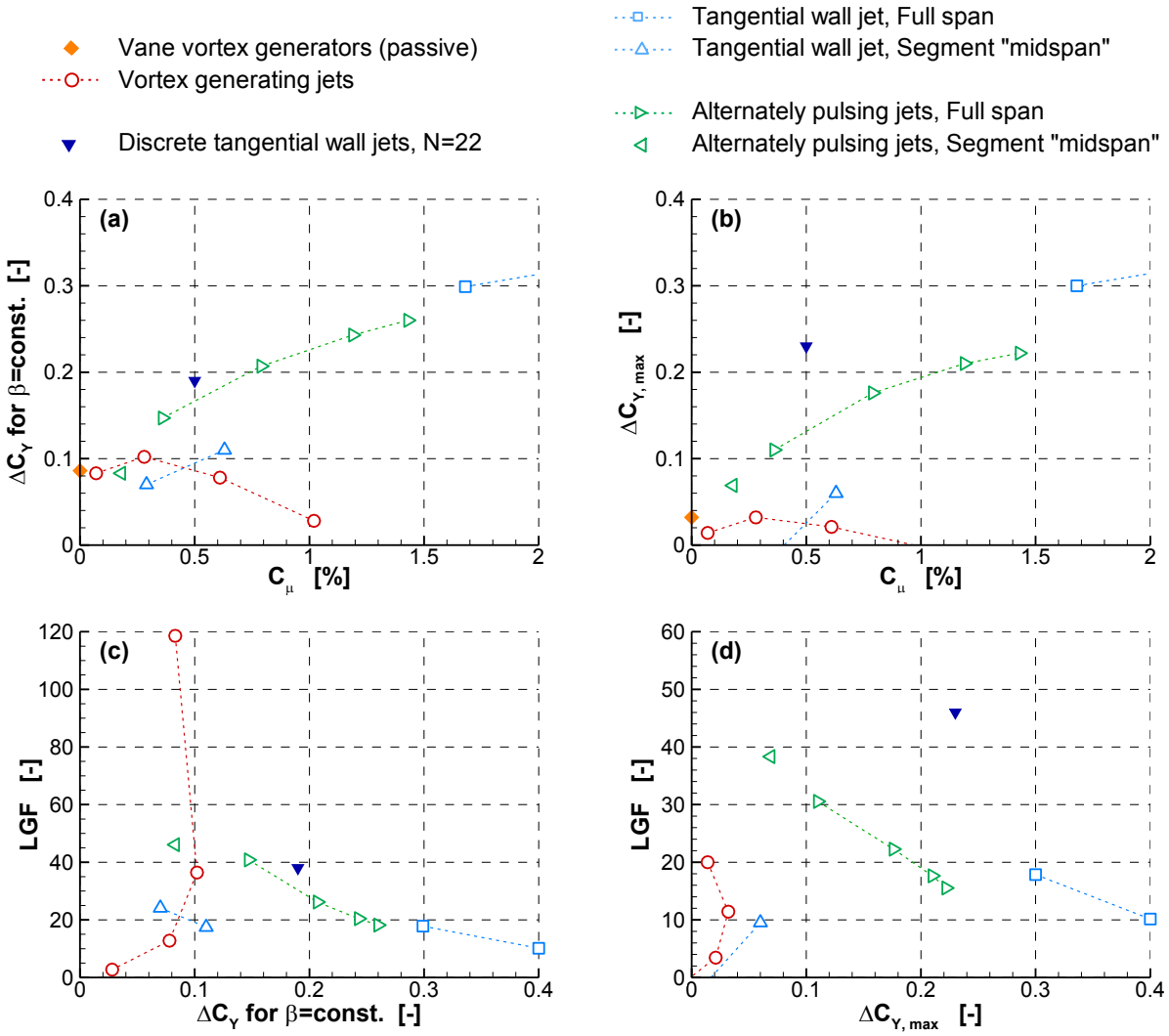

FIG. 10: Effectiveness and efficiency of the various methods compared with different approaches:
Subfigures (a) and (b) is the additional side force ΔC_Y that can be added with certain C_μ,
Subfigures (c) and (d) shows the efficiency in terms of the "Lift Gain Factor" LGF, eqn. (2),
Subfigures (a) and (c) assess the additional side force for a constant β in the linear region,
Subfigures (b) and (d) show the increase of the maximum side force relative to $C_{Y,max,Ref}$

5. CONCLUSIONS & SUMMARY

Different active flow control methods were studied comparatively to reveal their relative performance to control the flow separation on a generic vertical tail plane and gain higher side force. As an overview, each method was introduced with some characteristic results. All individual results are published elsewhere and the interested reader can find more details in the respective references. The focus of the present contribution is the comparison of the effectiveness and efficiency of the active methods.

The vortex generating jets are suitable, if a small increase of side force is required. The jets can create a vortex with comparatively low jet velocity and the jet exits have small cross sectional area, such that mass flow and C_μ, respectively, are small. For small effect, i.e. low ΔC_Y at low C_μ, and if β is below β_{max}, the vortex generating jets are clearly the most efficient method. It must also be noted that the VGJs are very easy to implement into the airfoil surface, requiring barely more than five holes and some tubing.

If larger side forces are required, the alternately pulsing jets are interesting. They can be used with anything between $C_\mu = 0.2$ % up to 1.5% and the gain in side force can effectively be varied over a wide range. The alternately pulsing jets can also easily be tuned to the required ΔC_Y or $\Delta C_{Y,max}$ by turning off individual elements over span, which was shown herein by discussing a case with only one segment at midspan being active and this case still offers a very good efficiency and a decent performance.

If very large additional side force in the excess of $\Delta C_Y > 0.3$ is required, only the tangential wall jet over the full span can generate it. However, it requires a significant amount of mass flow and, thus, has limited efficiency.

The discrete tangential wall jets seem to be a very interesting case, particularly for large β close to $C_{Y,max}$: This method is able to actually extend the usable β-range and since the required mass flow is much smaller than for a full span tangential wall jet, the efficiency is much higher. The parallel paper [11] will cover some more recent results regarding the discrete wall jets.

It should finally be noted that the study is not fully verified and crosschecked in all respects, yet: The data is taken from two different wind tunnels with different properties and also from numerical simulations. While the data for each method alone can be considered unbiased, the cross comparisons between the methods might not be fully transferable, since quantification of, both, C_μ and $C_{Y,max}$ is not straightforward. Future work will focus to secure the interpretations of the current results by experimentally testing the tangential wall jets, exchanging the different models between the wind tunnels, and by completing numerical simulations of the alternately pulsing jets and the vortex generating jets.

ACKNOWLEDGEMENTS

This contribution presents first core results that have been achieved in the collaborative research project AsSaM ("Autoritätssteigerung von Steuerflächen durch aktive Maßnahmen"), funded by the German Federal Ministry for Economics and Energy (BMWi) in the framework of the LuFo V ("Luftfahrtforschungsprogramm V") under grants 20E1513.

Cooperation and fruitful discussions with Bruno Stefes, Jean-Marc Hanke and Carsten Weber from Airbus Deutschland are gratefully acknowledged.

REFERENCES

[1] RATHAY, N.W., BOUCHER, M.J., AMITAY, M., WHALEN, E.A., Performance Enhancement of a Vertical Tail Using Synthetic Jet Actuators, AIAA Journal, Vol. 52, No. 4, pp. 810-820., 2014

[2] WHALEN, E.A., LACY, D., LIN, J.C., ANDINO, M.Y. et al., Performance Enhancement of a Full-Scale Vertical Tail Model Equipped with Active Flow Control, AIAA Paper 2015-0784, 53rd AIAA Aerospace Sciences Meeting, 2015

[3] LIN, J.C., ANDINO, M.Y., ALEXANDER, M.G., WHALEN, E.A., SPOOR, M.A., TRAN, J.T., WYGNANSKI, I.J., An Overview of Active Flow Control Enhanced Vertical Tail Technology Development, AIAA Paper 2016-0056, 54th AIAA Aerospace Sciences Meeting, 2016

[4] LACHMANN, G.V., Boundary Layer and Flow Control. Its Principles and Application, Pergamon Press, 1961

[5] ENGLAR, R.J., Circulation Control for High Lift and Drag Generation on STOL Aircraft, AIAA Journal of Aircraft, Vol. 12, No. 5, pp. 457-463, 1975

[6] JOSLIN, R.D., JONES, G.S., Applications of Circulation Control Technology, Progress in Astronautics and Aeronautics, AIAA, 2006

[7] RADESPIEL, R., BURNAZZI, M., CASPER, M., SCHOLZ, P., Active flow control for high lift with steady blowing, The Aeronautical Journal, Vol. 120, Special Issue 1223, S. 171-200, 2016

[8] KRÖHNERT, A., Numerical Investigation of Tangential Blowing at the Rudder of a Vertical Tailplane Airfoil, AIAA Paper 2014-2143, 32nd Applied Aerodynamics Conference, 2014

[9] GEBHARDT, A., Numerical Investigation of Unsteady Blowing Through Discrete Slots on a Swept Vertical Tail of Infinite Span, AIAA Paper 2017-3244, 35th AIAA Applied Aerodynamics Conference, 2017

[10] MEUNIER, M., BRUNET, V., High-lift devices performance enhancement using mechanical and air-jet vortex generators, AIAA Journal of Aircraft, Vol. 45, No. 6, pp 2049-2061, 2008

[11] GEBHARDT, A., Numerical Investigation of Tangential Blowing over the Rudder of a Vertical Tailplane, DGLR Paper 2018-0077, Deutscher Luft- und Raumfahrtkongress, 2018

[12] TAYLOR, H.D., The Elimination of Diffuser Separation by Vortex Generators. Rep. R-4012-3, United Aircraft Corp. Res. Dept., 1947

[13] McCURDY, W.J., Investigation of Boundary Layer Control of an NACA 16-325 Airfoil by Means of Vortex Generators. Rep. M-15038-3, United Aircraft Corp. Res. Dept., 1948

[14] JOHNSTON, J.P., NISHI, M., Vortex generator jets – Means for flow separation control. AIAA Journal, Vol. 28, No. 6, pp 989-994, 1990

[15] SINGH, V., SCHOLZ, P., Measurements on a Vertical Tail with Vane Vortex Generators, DGLR-ID 450111, Deutscher Luft- und Raumfahrtkongress, 2017

[16] SINGH, V., SCHOLZ, P., Comparison of Different Vortex Generating Devices for Flow Control on a Vertical Tail, AIAA Paper 2018-4023, AIAA Aviation Forum, 2018

[17] KATZ, Y., NISHRI, B., WYGNANSKI, I., The delay of turbulent boundary layer separation by oscillatory active control, Physics of Fluids A: Fluid Dynamics 1, Vol. 179, 1989

[18] SEIFERT, A., BACHAR, T., KOSS, D., SHEPSHELOVICH, M., WYGNANSKI, I.J., Oscillatory Blowing: A Tool to Delay Boundary-Layer Separation, AIAA Journal, Vol. 33, No. 11, pp. 2052-2060, 1993

[19] GREENBLATT, D., WYGNANSKI, I.J., The control of flow separation by periodic excitation, Progress in Aerospace Sciences, Vol. 36, pp. 487-545, 2000

[20] GRUND, T., NITSCHE, W., Wind Tunnel and Flight Tests with Active Flow Control on a S10 Glider Configuration, In: Notes on Numerical Fluid Mechanics and Multidisciplinary Design,, Vol. 121, pp. 117-124, 2013

[21] LÖFFLER, S., STAATS, M., GRUND, T., WEISS, J., Increasing the Effectiveness of a Vertical Stabilizer by Combining Pulsed Jet Actuation at the Leading Edge and the Rudder Hinge Line, AIAA Paper 2018-2854, AIAA Aviation Forum, 2018

[22] CATTAFESTA III, L.N., SHEPLAK, M., Actuators for Active Flow Control, Annual Review of Fluid Mechanics, Vol.43, pp. 247-272, 2011

[23] STAATS, M., LÖFFLER, S., EBERT, C., GRUND, T., WEISS, J., A Fluidic Device for Active Flow Control: Simulation vs. Experiment with Emphasis on Application, AIAA Paper 2018-3336, 36th AIAA Applied Aerodynamics Conference, 2018